A Novel Traction Control for EV Based on Maximum Transmissible Torque Estimation

Dejun Yin, *Student Member*, *IEEE*, Sehoon Oh, *Member*, *IEEE*, and Yoichi Hori, *Fellow*, *IEEE*

***Abstract*— Controlling an immeasurable state with an indirect control input is a difficult problem faced in traction control of vehicles. Research on motion control of electric vehicles has progressed considerably, but traction control has not been so sophisticated and practical because of this difficulty. Therefore, this work takes advantage of the features of driving motors to estimate the maximum transmissible torque output in real time based on a purely kinematic relationship. An innovative controller which follows the estimated value directly and constrains the torque reference for slip prevention is then proposed. By analysis and comparison with prior control methods, the resulting control design approach is shown to be more effective and more practical both in simulation and on an experimental electric vehicle.**

***Index Terms*— Electric Vehicle, Traction Control, Anti-Slip, Maximum Transmissible Torque Estimation**

I. Introduction

DUE to the drastically increasing price of oil and the growing concern about global environmental problems, research on electric vehicles is drawing more and more attention, and significant improvements in power electronics, energy storage and control technology have been achieved[1]-[3].

From the viewpoint of motion control, compared with internal combustion engine vehicles, the advantages of electric vehicles can be summarized as follows [4]:

1) Quick torque generation
2) Easy torque measurement
3) Independently equipped motors for each wheel

The torque output of the motor can be easily calculated from the motor current. This merit makes it easy to estimate the driving or braking forces between tire and road surface in real time, which contributes a great deal to application of new control strategies based on road condition estimation. The independently equipped motors provide higher power/weight density, higher redundancy for safety and better dynamic performance [5]-[6].

By introducing computer control technology, vehicle chassis control systems have made significant technological progress over the last decade to enhance vehicle stability and handling performance in critical dynamic situations. Among these controllers are systems such as antilock braking system (ABS) [7]-[8], direct yaw control (DYC) system [9]-[11], integrated vehicle dynamic control system, etc. However, effective operation of each of these control systems is based on some basic assumptions, for example, the output torque being able to accurately work on the vehicle.

For this purpose, traction control, as a primary control for vehicles, is developed to ensure the effectiveness of the torque output. The key to traction control is anti-slip control, when the vehicle is driven or brakes on a slippery road, especially for light vehicles because they are more inclined to skid on slippery roads. Traction control must not only guarantee the effectiveness of the torque output to maintain vehicle stability, but also provide some information about tire-road conditions to other vehicle control systems. Moreover, a well-managed traction control system can cover the functions of ABS, because motors can generate deceleration torque as easily as acceleration torque [12]. Based on the core traction control, more complicated two-degree-of-freedom motion control for vehicles can be synthesized by introduction of some information on steering angle, yaw rate, etc. [13]-[14]. From the viewpoint of the relation between safety and cost, a more advanced traction control synthesis also means lower energy consumption.

However, actual vehicles present challenges to research on traction control. For example, the real chassis velocity is not available, and the friction force which drives the vehicle is immeasurable. Depending on whether chassis velocity is calculated, the control implementations for anti-slip control fall into two classes. In general traction control systems that need the chassis velocity, due to physical and economic reasons, the non-driven wheels are utilized to provide an approximate vehicle velocity. However, this method is not applicable when the vehicle is accelerated by 4WD systems or decelerated by brakes equipped in these wheels. For this reason, the accelerometer measurement is also used to calculate the velocity value, but it cannot avoid offset and error problems. Other sensors, e.g., optical sensors [15], sensors of magnetic

Manuscript received August 24, 2008; revised February 4, 2009; accepted f or publication February 8, 2009.

Dejun Yin is with the Department of Electrical Engineering, Graduate Scho ol of Engineering, University of Tokyo, Tokyo 113-8656, Japan (e-mail:yin@h orilab.iis.u-tokyo.ac.jp).

S. Oh and Y. Hori are with the Institute of Industrial Science, University of Tokyo, Tokyo 153-8505, Japan (e-mail:sehoon@horilab.iis.u-tokyo.ac.jp).

Color versions of one or more of the figures in this paper are available onli ne at http://ieeexplore.ieee.org.

Digital Object Identifier xx.xxxx/TIE.2009.xxxxxx

markers [16]-[17], etc., can also obtain the chassis velocity. However, they are too sensitive and reliant on the driving environment or too expensive to be applied in actual vehicles. Some anti-slip control systems [7]-[8], [18] try to realize optimal slip ratio controls according to the Magic Formula [19]. However, these systems not only need extra sensors for the acquisition of chassis velocity or acceleration, but are also more difficult to realize than expected, because the tuned algorithms and parameters for specific tire-road conditions are cannot adapt quickly to the significant variation in the instantaneous, immeasurable relationship between slip ratio and friction coefficient in different driving conditions.

On the other hand, some controllers, for example Model Following Control (MFC), do not need information on chassis velocity or even acceleration sensors. In these systems, the controllers only make use of torque and wheel rotation as input variables for calculation. Fewer sensors contribute not only to lower cost, but also higher reliability and greater independence from driving conditions, which are the most outstanding merits of this class of control systems. Accordingly, research on more practical and more sophisticated anti-slip control based on MFC continues until now. Sakai et al. proposed a primary MFC system for anti-slip control [20]. Saito et al. modified it and proposed a novel stability analysis to decide the maximum feedback gain, and furthermore, took the anti-slip control as a core subsystem and extended it to two-degree-of-freedom motion control [13]-[14]. Akiba et al. improved the control performance by introduction of back electromotive force, and added a conditional limiter to avoid some of its inherent drawbacks [21]. Nevertheless, these control designs based on compensation have to consider the worst stability case to decide the compensation gain, which impairs the performance of anti-slip control. Furthermore, gain tuning for some specific tire-road conditions also limits the practicability of this method.

Therefore, this paper, making use of the advantages of electric vehicles, focuses on development of a core traction control system based on Maximum Transmissible Torque Estimation (MTTE) that requires neither chassis velocity nor information about tire-road conditions. In this system, use is made of only the torque reference and the wheel rotation to estimate the maximum transmissible torque to the road surface, then the estimated torque is applied for anti-slip control

Fig. 1. COMS3-A new experimental electric vehicle.

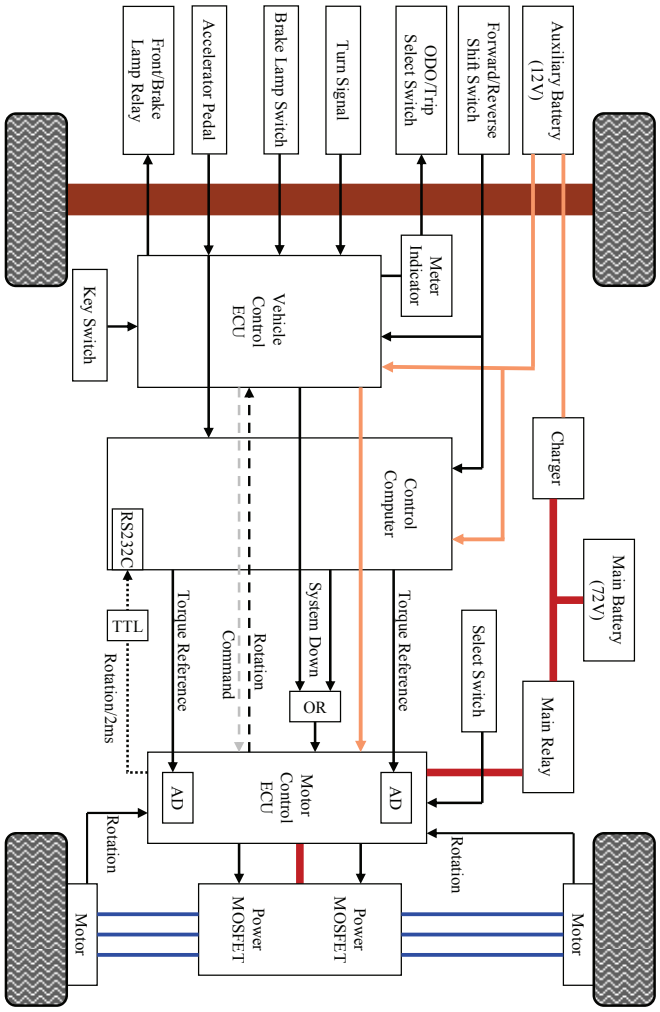

Fig. 2. Schematic of electrical system of COMS3.

implementation.

The rest of the paper is structured as follows. Section II describes an electric vehicle modified for experiments. Section III presents a longitudinal model of vehicles, and analyzes the features of anti-slip control. MTTE and a control algorithm based on it are then proposed. Comparing with MFC for anti-slip control, section IV demonstrates simulations and experiments. A detailed discussion follows in Section V, analyzing the features of the proposed control method.

II. Experimental Electric Vehicle

In order to implement and verify the proposed control system, a commercial electric vehicle, COMS, which is made by TOYOTA AUTO BODY Co. Ltd., shown in Fig. 1 was modified to fulfill the experiments' requirements. Each rear wheel is equipped with an Interior Permanent Magnet Synchronous Motor (IPMSM) and can be controlled independently.

As illustrated in Fig. 2, a control computer is added to take the place of the previous ECU to operate the motion control. The computer receives the acceleration reference signal from

TABLE I
SPECIFICATION OF COMS3

Total Weight	360kg
Max. Power	2000W × 2
Max. Torque	100Nm × 2
Wheel Inertia	0.5kgm^2 × 2
Wheel Radius	0.22m
Sampling Time	0.01s
Controller	PentiumM1.8G, 1GB RAM
A/D and D/A	12 bit
Shaft Encoder	36 pulse/round

the acceleration pedal sensor, the forward/backward signal from the shift switch and the wheel rotation from the inverter. Then, the calculated torque reference of the left and the right rear wheel are independently sent to the inverter by two analog signal lines. Table I lists the main specifications.

The most outstanding feature of the modified inverter is that the minimum refresh time of the torque reference is decreased from 10ms to 2ms, which makes it possible to actualize the torque reference more quickly and accurately. The increased maximum rate of change of the torque reference permits faster torque variation for high performance motion control.

III. MTTE FOR ANTI-SLIP CONTROL

A. Longitudinal Model and Dynamic Analysis

Because only longitudinal motion is discussed in this paper, the dynamic longitudinal model of the vehicle can be described as in Fig. 3, and the parameter definition is listed in Table II.

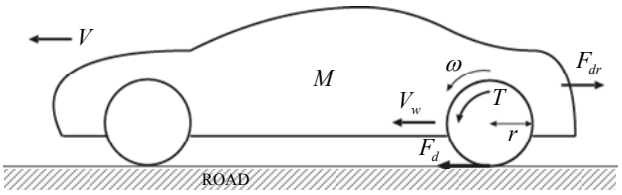

Fig. 3. Dynamic longitudinal model of vehicle.

Generally, the dynamic differential equations for the calculation of longitudinal motion of the vehicle are described as follows:

$$J_w\dot{\omega} = T - rF_d \tag{1}$$

$$M\dot{V} = F_d - F_{dr} \tag{2}$$

$$V_w = r\omega \tag{3}$$

$$F_d(\lambda) = \mu N \tag{4}$$

The interrelationships between the slip ratio and friction coefficient can be described by various formulas. Here, as shown in Fig. 4, the widely adopted Magic Formula is applied to build a vehicle model for the following simulations.

TABLE II
PARAMETER LIST

Symbol	Definition
J_w	Wheel Inertia
V_w	Wheel Velocity (Circumferential Velocity)
ω	Wheel Rotation
T	Driving Torque
r	Wheel Radius
F_d	Friction Force (Driving Force)
M	Vehicle Mass
N	Vehicle Weight
V	Chassis Velocity (Vehicle Velocity)
F_{dr}	Driving Resistance
λ	Slip Ratio
μ	Friction Coefficient

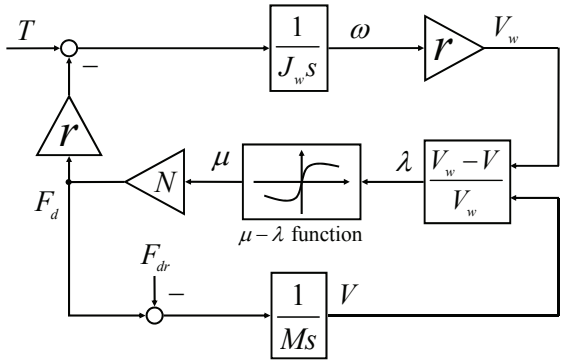

Fig. 4. One wheel vehicle model with Magic Formula.

B. Maximum Transmissible Torque Estimation

In this paper, in order to avoid the complicated μ-λ relation, only the dynamic relation between tire and chassis is considered based on the following considerations, which transform the anti-slip control into maximum transmissible torque control.

1) Whatever kind of tire-road condition the vehicle is driven in, the kinematic relationship between the wheel and the chassis is always fixed and known.
2) During the acceleration phase, considering stability and tire abrasion, well-managed control of the velocity difference between wheel and chassis is more important than the mere pursuit of absolute maximum acceleration.
3) If the wheel and the chassis accelerations are well controlled, the difference between the wheel and the chassis velocities, i.e. the slip is also well controlled.

According to (1) and (3), the driving force, i.e. the friction force between the tire and the road surface, can be calculated as (5). Assuming T is constant, it can be found that the higher V_w, the lower F_d. In normal road conditions, F_d is less than the

maximum friction force from the road and increases as T goes up. However, when slip occurs, F_d equals the maximum friction force that the tire-road relation can provide and cannot increase with T. Here, there are only two parameters, r and J_w, so F_d is easily calculated in most tire-road conditions.

$$F_d = \frac{T}{r} - \frac{J_w \dot{V}_w}{r^2} \tag{5}$$

When slip starts to occur, the difference between the velocities of the wheel and the chassis become larger and larger, i.e. the acceleration of the wheel is larger than that of the chassis. Furthermore, according to the Magic Formula, the difference between the accelerations will increase with the slip.

Therefore, the condition that the slip does not start or become more severe is that the acceleration of the wheel is close to that of the chassis. Moreover, considering the μ-λ relation described in the Magic Formula, an appropriate difference between chassis velocity and wheel velocity is necessary to provide the friction force. Accordingly, (6) defines α as a relaxation factor to describe the approximation between the accelerations of the chassis and the wheel. In order to satisfy the condition that slip does not occur or become larger, α should be close to 1.

$$\alpha = \frac{\dot{V}^*}{\dot{V}_w^*}, \text{ i.e. } \alpha = \frac{(F_d - F_{dr})/M}{(T_{\max} - rF_d)r/J_w} \tag{6}$$

With a designed α, when the vehicle enters a slippery road, $T_{\max}$ must be reduced adaptively following the decrease of F_d to satisfy (6), the no-slip condition.

Since the friction force from the road is available from (5), the maximum transmissible torque, $T_{\max}$ can be calculated as (7). This formula indicates that a given F_d allows a certain maximum torque output from the wheel so as not to increase the slip. Here, it must be pointed that driving resistance, F_{dr} is assumed to be 0, which will result in an over evaluation of $T_{\max}$ and consequently impair the anti-slip performance. However, F_{dr} is a variable related with the chassis velocity and the vehicle shape, and can be calculated or estimated in real time if higher anti-slip performance is required or if the vehicle runs at high speed [22]-[24]. Although the vehicle mass, M can also be estimated online [25]-[28], in this paper it is assumed to be constant.

$$T_{\max} = \left(\frac{J_w}{\alpha M r^2} + 1 \right) r F_d \tag{7}$$

Finally, the proposed controller can use $T_{\max}$ to constrain the torque reference if necessary.

C. Controller Design

The torque controller is designed as in Fig. 5, in which the limiter with a variable saturation value is expected to realize the control of torque output according to the dynamic situation. Under normal conditions, the torque reference is expected to pass through the controller without any effect. On the other hand, when on a slippery road, the controller can constrain the torque output to be close to $T_{\max}$.

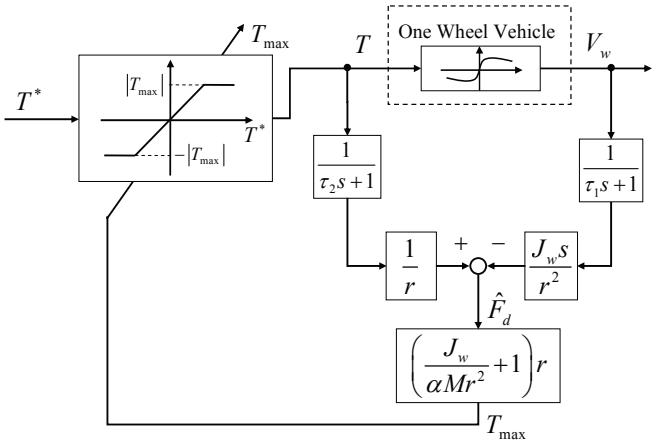

Fig. 5. Control system based on MTTE.

Firstly, the estimator uses the commanded torque into the inverter and the rotation speed of the wheel to calculate the friction force, and then estimates the maximum transmissible torque according to (7). Finally, the controller utilizes the estimated torque value as a saturation value to limit the torque output. In essence, the estimation shown in Fig. 5 is a disturbance observer.

Here, although it will cause some phase shift, duo to the low resolution of the shaft encoder installed in the wheel, a low pass filter (LPF) with a time constant of τ_1 is introduced to smooth the digital signal, V_w, for the differentiator which follows. In order to keep the filtered signals in phase, another LPF with a time constant of τ_2 is added for T.

D. Stability Analysis

Considering that the Magic Formula included in the vehicle model shown in Fig. 4 is non-linear, the paper makes use of an equivalent model [13]-[14] for stability analysis to decide parameters.

Slip occurs when part of the outputted torque can not be transmitted to the chassis by the tire-road interaction, resulting in lower chassis acceleration than that of wheel. Here, (8) uses Δ to describe the ratio of the under-transmitted torque. In addition, taking into account the ideal state and the worst slip case in which the wheel spins completely idly, i.e. the inertia of the whole system equals to the inertia of wheel, J_w, the variation range of Δ is available too.

$$\dot{V} - \dot{V}_w = -\frac{\Delta T}{Mr}, \ \Delta \in [0, \ Mr^2/J_w] \tag{8}$$

According to (1), (2) and (8), the dynamic longitudinal model of the vehicle can be simplified as in (9), a SISO system that masks the complicated interaction among tire, chassis and road, which contributes to the stability analysis. That is, the unwanted wheel acceleration that causes slip can be regarded as the result of a decrease in system inertia. And, Δ can also be treated as a description of variation in system inertia.

$$J\dot{\omega} = T \tag{9}$$

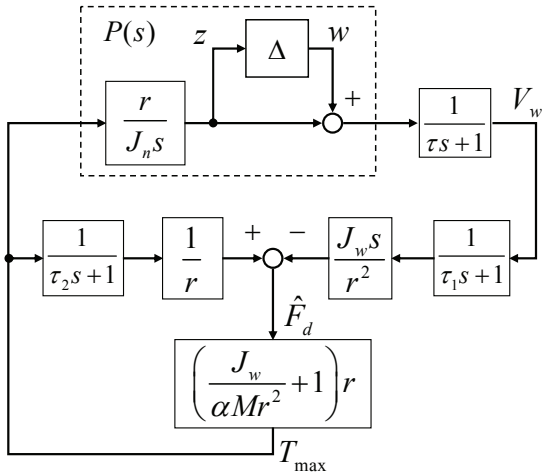

Fig. 6. Equivalent closed-loop control system.

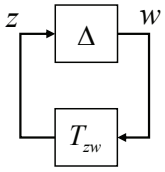

Fig. 7. Equivalent block diagram. Here, T_{zw} is the transfer function from w to z in Fig. 6.

Here, as shown in (10), J is the equivalent inertia of the whole vehicle system from the viewpoint of the driving wheel, and J_n the nominal inertia where no slip occurs.

$$J = \frac{J_n}{1+\Delta},\ J_n = J_w + Mr^2 \tag{10}$$

Consequently, use is made of (9) to take place of the vehicle model shown in Fig. 5 for stability analysis. When the vehicle rapidly accelerates on a slippery road, the estimated $T_{\max}$ will constrain T^* and take its place to be treated as the input value to the motor. In this case, the whole system will automatically transform into a closed feedback system, as shown in Fig. 6. Here, in order to analyze the stability easily, the delay of the electro-mechanical system is simplified as a LPF with a time constant of τ.

Fig. 7, as the equivalent block diagram of Fig. 6, is used for the analysis of the closed-loop stability against Δ, the model variation. T_{zw} in Fig. 7 is described in (12).

$$T_{zw} = \frac{-J_w K}{J_n r\tau\tau_1 s^2 + J_n((r-K)\tau + r\tau_1)s + J_n r - Mr^2 K} \tag{12}$$

Here,

$$K = \left(\frac{J_w}{\alpha Mr^2} + 1\right) r \tag{13}$$

As a result, the following conditions in (15) must be satisfied to ensure the closed-loop stability, i.e., ensure the real part of the roots of the characteristic equation (14) to be negative [29].

Here, τ_2 is assumed equal to τ_1 to simplify the solution.

$$1 - T_{zw}\Delta = 0 \tag{14}$$

$$\begin{cases} K < \dfrac{Mr^2 + J_w}{Mr^2 - \Delta J_w} r \\ \tau_1 > \dfrac{K-r}{r}\tau \end{cases}, \text{ i.e. } \begin{cases} \alpha > \dfrac{1 - J_w\Delta / Mr^2}{1+\Delta} \\ \tau_1 > \dfrac{J_w \tau}{\alpha Mr^2} \end{cases} \tag{15}$$

It can be found in (15) that if there is no limiter, when the vehicle runs in a normal state, α must be larger than 1 to fulfill the requirement for stability. However, considering (7), when α is larger than 1, $T_{\max}$ will be always restrained to be smaller than the torque that the tire-road interface can provide, which will impair the acceleration performance.

Therefore, in this paper, α is designed to be slightly smaller than 1 to ensure acceleration performance while improving the anti-slip performance.

E. Compensation for Acceleration Performance

In real experiments, even in normal road conditions, $T_{\max}$ may be smaller than T^* due to system delay at the acceleration start, which will cause suddenly commanded acceleration to be temporarily constrained by $T_{\max}$ during the acceleration phase.

In order to avoid this problem, the increasing rate of T^* is amplified as a stimulation to make the under evaluated $T_{\max}$ to meet the acceleration reference. Here, $T'_{\max}$ is used instead of $T_{\max}$ as the input to the controller, whose relation is described by (16). Here, G is a compensation gain. Additionally, the over expanded $T'_{\max}$ can be automatically constrained by the following controller.

$$T'_{\max} = T_{\max} + \dot{T}^* G \ (\dot{T}^* > 0) \tag{16}$$

IV. Simulation And Experimental Results

A. MFC for Anti-slip control

This paper uses the anti-slip control system based on MFC presented in [13] and [14], shown in Fig. 8, for the following comparison.

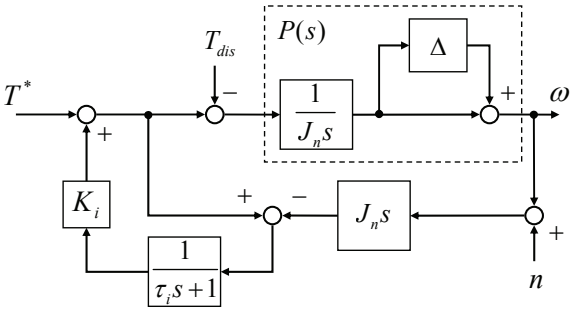

Fig. 8. Block diagram of MFC for slip prevention.

K_i, shown in (16), must fulfill the condition for robust stability. Considering the worst slip case, K_{im} is used to represent the maximum feedback gain that ensures robust

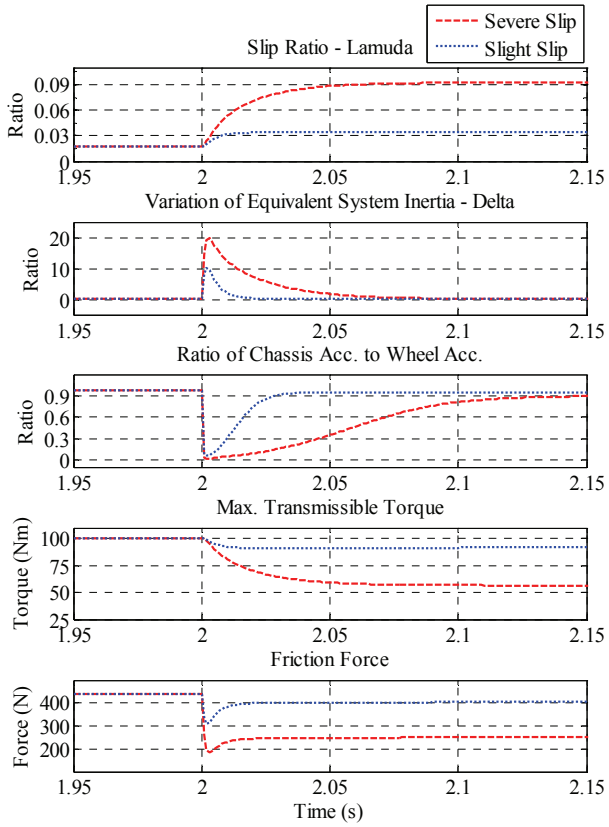

Fig. 9. Anti-slip performance and system stability when α=0.9. In the simulation of severe slip, the maximum friction coefficient is set to 0.3, and slight slip 0.6. Here, commonly used λ and Δ are utilized to describe the extent of slip.

stability.

$$K_i < \frac{1}{\Delta},\ \Delta \in [0,\ Mr^2/J_w] \tag{16}$$

$$K_{im} = \frac{J_w}{Mr^2} \tag{17}$$

In the following simulations and experiments, the same parameters of the vehicle are adopted for comparison, and τ_i is equal to τ_1.

B. Simulation Results

Simulation systems were synthesized based on the model of Fig. 5 and Fig. 8 respectively.

Fig. 9 illustrates the stability of the control system in which α is designed to be smaller than 1 for two different slip states. In this simulation, the system delay is shortened to make the primary tendency clear.

Fig. 10 and Fig. 11 show the simulation results with variation in α and τ_1. Additionally, Fig. 12 provides the simulation results of MFC for comparison. The maximum friction coefficient of the slippery road is 0.3. Here, τ_1, τ_2 and τ_i are set to 50 ms, and τ=40 ms.

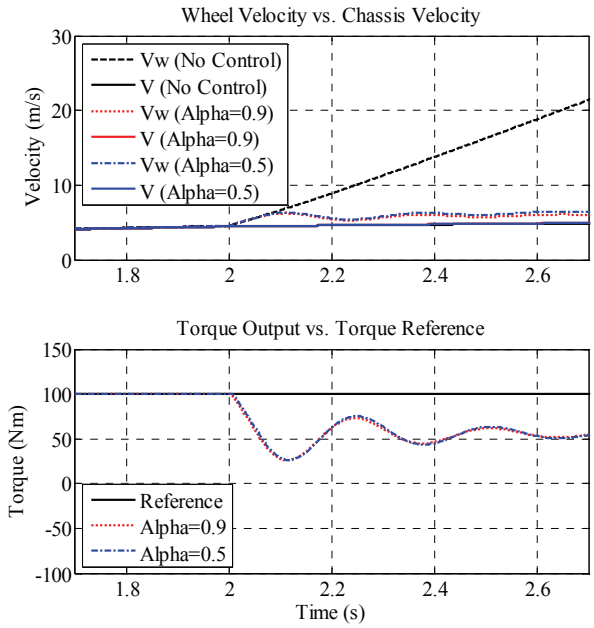

Fig. 10. Comparison of simulation results with variation in α.

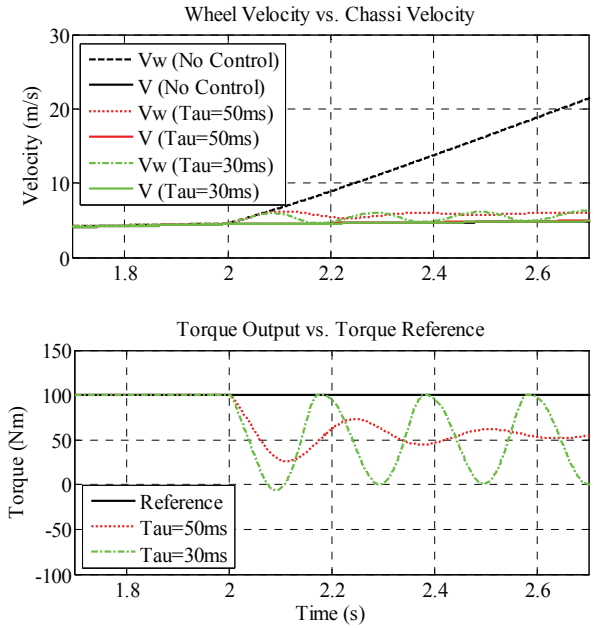

Fig. 11. Comparison of simulation results with variation in τ_1.

C. Experiment Results

Controllers designed based on the simulated algorithm were applied to COMS3 for experiments. In these experiments, the slippery road was simulated by an acrylic sheet with a length of 1.2m and lubricated with water. The initial velocity of the vehicle was set higher than 1m/s to avoid the immeasurable zone of the shaft sensors installed in the wheels.

Here, it must be pointed out that in order to detect the chassis velocity, only the left rear wheel is driven by the motor, while the right rear wheel rolls freely to provide a reference value of the chassis velocity for comparison.

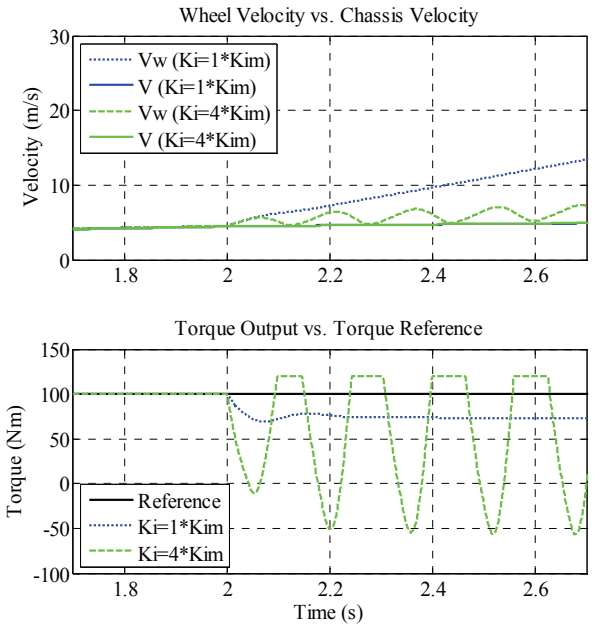

Fig. 12. Comparison of simulation results of MFC with variation in K_i. Although the largest K_i for stability is K_{im}, the simulation result of $K_i = 4*K_{im}$ is shown for comparison.

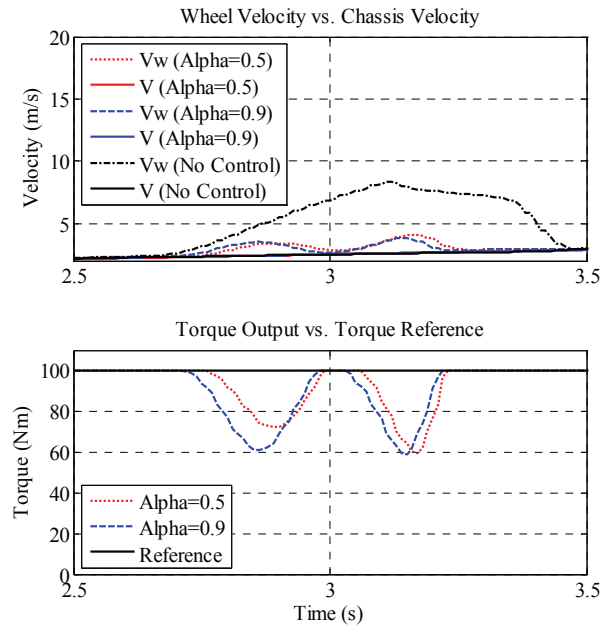

Fig. 13. Comparison of experiment results with variation in α. In this experiment, τ_1 and τ_2 are fixed as 50ms.

Fig. 13 and Fig. 14 show the experimental results with variation in α and τ_1, and Fig. 15 the results using MFC for comparison. Fig. 16 illustrates the performance of acceleration compensation with G=0.1.

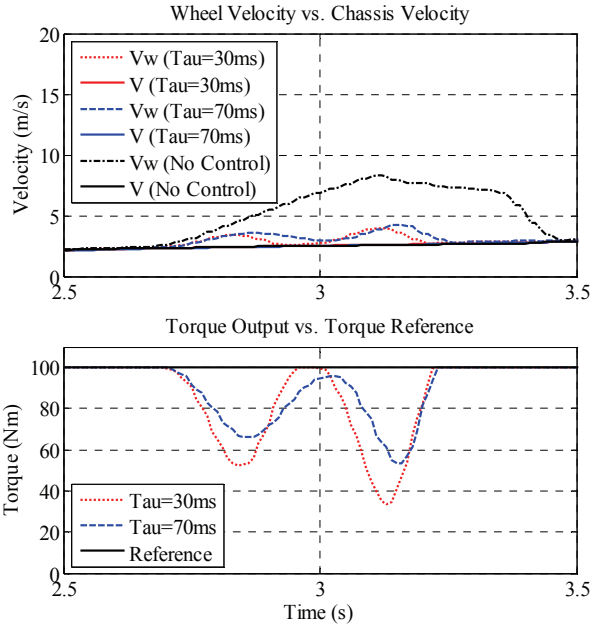

Fig. 14. Comparison of experiment results with variation in τ_1. In this experiment, α is fixed at 0.9.

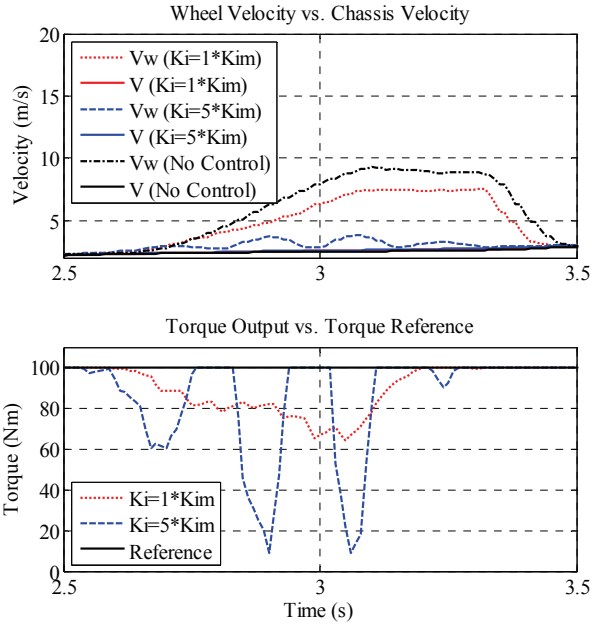

Fig. 15. Comparison of simulation results of MFC with variation in K_i.

V. Discussion

A. Relaxation Factor and Stability

When α is smaller than 1, according to (1) and (7), it can be found that when the vehicle runs in no-slip conditions, as described as (18), T_{max} will be larger than T^*, and the unwanted torque will be eliminated by the limiter, which keeps the system stable and responsive to the driver's torque reference.

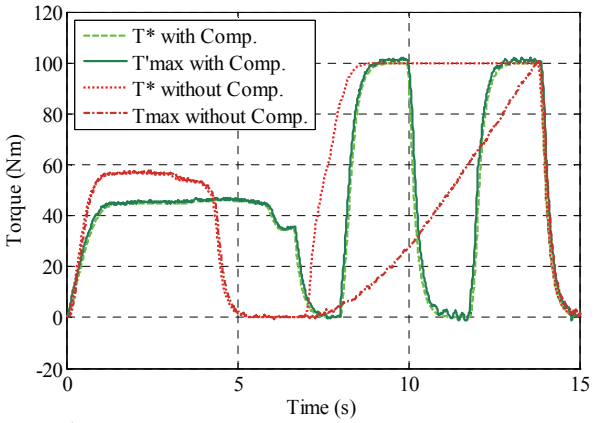

Fig. 16. T^* vs. $T_{\max}$ in experiments with/without compensation.

$$T_{\max} = T + \frac{J_w}{r}\left(\frac{1}{\alpha}\dot{V} - \dot{V}_w\right) \tag{18}$$

On the other hand, when the vehicle enters a slippery road, as described in Fig. 9, due to the system delay, a sudden slip will occur at the first, and then, the whole system will work in two different states:

1) Slight slip that makes (15) valid, i.e. the system is theoretically unstable. However, a well designed α will allow $T_{\max}$ to rise to increase the slip properly, according to the Magic Formula, so as to provide an increased friction force, as expected.

2) Severe slip that satisfies (15) occurs. System is stable, i.e. $T_{\max}$ will become smaller and smaller to restrain the slip. The ratio of the acceleration of the chassis to that of the wheel will become larger and larger to meet the designed α.

In conclusion, the simulations and experiments indicate that, a relaxation factor α which is smaller than 1 makes the system work at a critical state, which results in the best anti-slip performance while keeping system stable.

B. *Performance of the proposed anti-slip control*

Fig. 10 and Fig. 13 show that, compared to the no-control case, the difference between the wheel velocity and the chassis velocity caused mainly by the delay in the control system does not increase. The estimated maximum transmissible torque is close to the input reference torque in the normal road, and corresponds to the maximum friction force allowed by the slippery tire-road surface.

The results also indicate that the larger α, the better anti-slip performance. A larger relaxation factor further limits the difference between the accelerations of the chassis and the wheel. In fact, when the control system falls into an anti-slip state, it also transforms into a closed feedback system shown as Fig. 17. Here, D represents the extent of the slip, and the relation between D and F_d is not considered. The transfer function from F_d to D indicates the effect of α in (19).

$$\frac{D}{F_d} = \frac{-\alpha(J_w + Mr^2)[\tau\tau_1 s^2 + (\tau+\tau_1)s] + J_w(1-\alpha)}{\alpha J_w M[\tau\tau_1 s^2 + (\tau+\tau_1)s + 1]s} \tag{19}$$

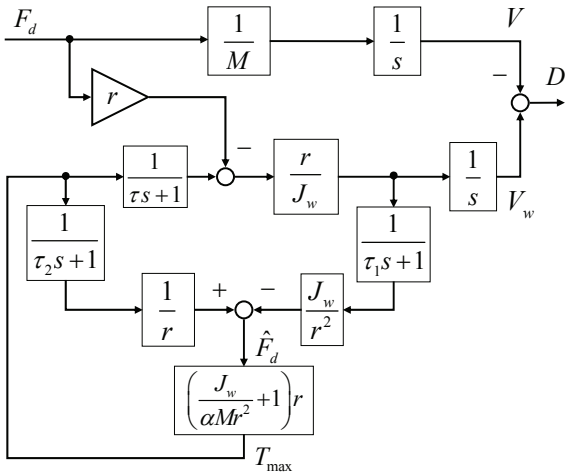

Fig. 17. Equivalent closed-loop control system without consideration of the μ-λ relation.

Fig. 11 and Fig. 14 show that an insufficiently large value of τ_1, especially when it is smaller than the delay time of the electromechanical system, can cause the control system to become unstable, and result in more severe torque oscillation, which makes driving operation feel rough. However, a larger time constant in the LPF means a larger phase shift that results in more severe slip at start of slip.

C. *Comparison with MFC*

Fig. 12 and Fig. 15 show that, compared with the control based on MTTE, MFC cannot provide a good tradeoff between anti-slip performance and control stability. With K_{im}, the largest feedback gain that ensures system stability for any slip state, the control synthesis can not constrain the slip as expected. With a much larger K_{i}, the control synthesis succeeded in constraining the slip, but the torque output was too oscillatory. The experiments also showed that, even in normal conditions, MFC with a large feedback gain can cause system instability.

Additionally, although a well-tuned K_{i} can make a good tradeoff for a specific tire-road condition, such a system will become unstable in more slippery conditions, which limits the practicality of this method.

On the other hand, with a different control philosophy, the proposed control based on MTTE does not depend on the error between the expected output and the real output to decide the control output, but follows the estimated load directly to calculate the control input, i.e. according to its needs, which contributes to higher control performance and higher applicability in any tire-road condition. From this viewpoint, the proposed control topology can be called Load Following Control.

Compared with other control systems, the proposed control has some other merits. The driver can directly control the acceleration at any time, because the driver will be given the priority to take back the control of the motor from the controller immediately only if T^* becomes smaller than $T_{\max}$. In addition, MTTE can not only provide $T_{\max}$ for anti-slip control in critical

situations, but also inform other vehicle control systems of the tire-road situation.

D. Compensation

Fig. 16 shows that the deterioration of pedal response caused by large system delay may occur in the control system without compensation. In this case, the control system must take a long time to restore direct control of acceleration to the driver. The experiments also indicate that without this compensation, for higher α, loss of control occurs more frequently.

However, the additional increasing rate of T^* provides compensation to follow the acceleration reference, avoiding this problem. In fact, if T^* remains constant, the compensation will not affect anti-slip control performance.

VI. Conclusion

This paper proposed an estimator of maximum transmissible torque and applied it to the control of the driving motors in electric vehicles for slip prevention.

This estimator, which does not calculate chassis velocity, instead using only the input torque and output rotation of the wheel, provides a good foundation for anti-slip control. The effectiveness of the estimation showed that motors can act not only as actuators but also as a good platform for state estimation because of their inherently fast and accurate torque response. The experiments and simulations verified the effectiveness of the estimation in anti-slip control. Additionally, this estimator is also expected to provide the maximum transmissible torque for other vehicle control systems to enhance their control performance when the vehicle runs in slippery conditions.

The controller designed to co-operate with the estimator can provide higher anti-slip performance while maintaining control stability. When excessive torque is commanded, this controller constrains the control output to follow the actual maximum driving force between the tire and the road surface, which provides high adaptability to the control system in different tire-road conditions. In addition, the acceleration compensation resolved the problem of deterioration of pedal response due to system delay.

Comparative experiments and simulations with variation of control variables proved the effectiveness and practicality of the proposed control design.

Acknowledgment

The authors wish to thank the engineers at AISIN AW CO., LTD. for their cooperation on the inverter modification; Eric Wu of Keio University for advice and language check for the manuscript. This research was supported by the Global COE in Secure-Life Electronics, the University of Tokyo.

References

[1] K. T. Chau, C. C. Chan, and Chunhua Liu, "Overview of Permanent-Magnet Brushless Drives for Electric and Hybrid Electric Vehicles", *IEEE Transaction on Industrial Electronics*, Vol. 55, No. 6, pp. 2246-2257, 2008.

[2] Antonio Affanni, Alberto Bellini, Giovanni Franceschini, Paolo Guglielmi, and Carla Tassoni, "Battery Choice and Management for New-Generation Electric Vehicles", *IEEE Transaction on Industrial Electronics*, Vol. 52, No. 5, pp.1343-1349, 2005.

[3] Masao Nagai, "The perspectives of research for enhancing active safety based on advanced control technology", *Vehicle System Dynamics*, Vol. 45, No. 5, pp.413-431, 2007.

[4] Yoichi Hori, "Future Vehicle Driven by Electricity and Control -Research on Four-Wheel-Motored "UOT Electric March II", *IEEE Transaction on Industrial Electronics*, Vol. 51, No. 5 pp.954-962, 2004.

[5] Peng He and Yoichi Hori, "Optimum Traction Force Distribution for Stability Improvement of 4WD EV in Critical Driving Condition", *IEEE International Workshop on Advanced Motion Control*, pp.596-601, 2006.

[6] Nobuyoshi Mutoh, Yusuke Takahashi, and Yoshiki Tomita, "Failsafe Drive Performance of FRID Electric Vehicles With the Structure Driven by the Front and Rear Wheels Independently", *IEEE Transaction on Industrial Electronics*, Vol. 55, No. 6, pp. 2306-2315, 2008.

[7] Michael Schinkel and Ken Hunt, "Anti-Lock Braking Control using a Sliding Mode like Approach", *Proceedings of the American Control Conference*, Vol. 3, pp.2386-2391, 2002.

[8] Chinmaya B. Patil, Raul G. Longoria, and John Limroth, "Control prototyping for an anti-lock braking control system on a scaled vehicle", *Proceedings of the IEEE Conference on Decision and Control*, Vol. 5, pp. 4962-4967, 2003.

[9] Farzad Tahami, Shahrokh Farhangi, and Reza Kazemi, "A Fuzzy Logic Direct Yaw-Moment Control System for All-Wheel-Drive Electric Vehicles", *Vehicle System Dynamics*, Vol. 41, No. 3, pp.203-221, 2004.

[10] Takuya Mizushima, Pongsathorn Raksincharoensak, and Masao Nagai, "Direct Yaw-moment Control Adapted to Driver Behavior Recognition", *SICE-ICASE International Joint Conference 2006*, pp. 534-539, 2006.

[11] Massimo Canale, Lorenzo Fagiano, Antonella Ferrara, and Claudio Vecchio, "Vehicle Yaw Control via Second-Order Sliding-Mode Technique", *IEEE Transactions on Industrial Electronics*, Vol. 55, No. 11, pp.3908-3916, 2008.

[12] Nobuyoshi Mutoh, Yuichi Hayano, Hiromichi Yahagi, and Kazuya Takita, "Electric Braking Control Methods for Electric Vehicles With Independently Driven Front and Rear Wheels", *IEEE Transaction on Industrial Electronics*, Vol. 54, No. 2, pp.1168-1176, 2007.

[13] Takeo Saito, Hiroshi Fujimoto, and Toshihiko Noguchi, "Yaw-Moment Stabilization Control of Small Electric Vehicle", *Industrial Instrumentation and Control, IEE Japan*, pp.83-88, 2002.

[14] Hiroshi Fujimoto, Takeo Saito, and Toshihiko Noguchi, "Motion Stabilization Control of Electric Vehicle under Snowy Conditions Based on Yaw-Moment Observer", *IEEE International Workshop on Advanced Motion Control*, pp.35-40, 2004.

[15] J. D. Turner and L. Austin, "Sensors for Automotive Telematics", *Measurement Science & Technology*, Vol. 11, No. 2, pp. R58-79, 2000.

[16] Hyeongcheol Lee and Masayoshi Tomizuka, "Adaptive Vehicle Traction Force Control for Intelligent Vehicle Highway Systems (IVHSs)", *IEEE Transaction on Industrial Electronics*, Vol. 50, No. 1, pp.37-47, 2003.

[17] Shashikanth Suryanarayanan, and Masayoshi Tomizuka, "Appropriate Sensor Placement for Fault-Tolerant Lane-Keeping Control of Automated Vehicles", *IEEE/ASME Transactions on Mechatronics*, Vol. 12, No. 4, pp.465-471, 2007.

[18] Kiyoshi Fujii and Hiroshi Fujimoto, "Traction control based on slip ratio estimation without detecting vehicle speed for electric vehicle", *Fourth Power Conversion Conference-NAGOYA*, pp.688-693, 2007.

[19] Hans B. Pacejka and Egbert Bakker, "The Magic Formula Tyre Model", *Vehicle System Dynamics*, Vol. 21, No. 1, pp.1-18, 1992.

[20] Shin-ichiro Sakai and Yoichi Hori, "Advantage of Electric motor for anti skid control of electric vehicle", *European Power Electronics Journal*, vol. 11, No. 4, pp.26-32, 2001.

[21] Toru Akiba, Ryota Shirato,Takeshi Fujita and Jun Tamura, "A study of Novel Traction Control Model for Electric Motor Driven Vehicle", *4th Power Conversion Conference-NAGOYA*, Conference Proceedings, pp.699-704, 2007.

[22] Shin-ichiro Sakai, Hideo Sado, and Yoichi Hori, "Motion Control in an Electric Vehicle with 4 Independently Driven In-Wheel Motors", *IEEE Transaction on Mechatronics*, vol.4, No.1, pp.9-16, 1999.

[23] Jun-Yi Cao, Bing-Gang Cao, and Zhong Liu, "Driving Resistance Estimation Based on Unknown Input Observer", *Journal of Applied Sciences*, pp.888-891, 2006.

[24] K. Fujii and H. Fujimoto, "Slip Ratio Estimation and Control based on Driving Resistance estimation without Vehicle Speed Detection for Electric Vehicle", *The Society of Instrument and Control Engineers*, Conference Proceeding, 2007.

[25] Ikeda M., Ono T., and Aoki N., "Dynamic mass measurement of moving vehicles", *Transactions of the Society of Instrument and Control Engineers*, Vol. 28, No. 1, pp. 50-58, 1992.

[26] A. Vahidi, A. Stefanopoulou, and H. Peng, "Recursive least squares with forgetting for online estimation of vehicle mass and road grade: theory and experiments", *Vehicle System Dynamics*, pp.31-55, 2005.

[27] Vincent Winstead and Ilya V. Kolmanovsky, "Estimation of Road Grade and Vehicle Mass via Model PredictiveControl", *IEEE Conference on Control Applications*, Conference Proceeding, WC2.3, 2005.

[28] Ratiroch-Anant Phornsuk, Hirata Hiroshi, Anabuki Masatoshi, and Ouchi Shigeto, "Adaptive controller design for anti-slip system of EV", *2006 IEEE Conference on Robotics, Automation and Mechatronics*, pp. 4018749, 2006.

[29] Petros A. Ioannou and Jing Sun, "Robust Adaptive Control", *Prentice Hall*, pp.79-104, 1995.

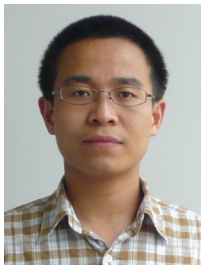

Dejun Yin (S'08) received the B.S. and M.S. degrees in electrical engineering from Harbin Institute of Technology, Harbin, China in 1999 and 2001 respectively. He received another M.S. degree in electronics engineering from Chiba Institute of Technology, Japan, in 2002, where he worked on embedded control system design in mechanical-electronics engineering for nearly 5 years.

He is currently a doctoral candidate in electrical engineering at the University of Tokyo, Japan, performing research on the development of motion control for electric vehicles. He is a member of the Institute of Electrical Engineers of Japan and the Society of Automotive Engineers of Japan.

Sehoon Oh (S'05-M'06) received the B.S., M.S. and Ph.D. degrees in Electrical Engineering from the University of Tokyo in 1998, 2000 and 2005, respectively. He is now working in the Institute of Industrial Science, the University of Tokyo as a Designated Research Associate.

His research fields are development of human-friendly motion control algorithm and assistive devices for people. He is a member of the Institute of Electrical Engineers of Japan (IEE-Japan), the Society of Instrument and Control Engineers (SICE), the Robotic Society of Japan (RSJ), and the Institute of Electric and Electronics Engineers (IEEE).

Yoichi Hori (S'81-M'83-SM'00-F'05) received the B.S., M.S., and Ph.D. degrees in electrical engineering from The University of Tokyo, Tokyo, Japan, in 1978, 1980, and 1983, respectively. In 1983, he joined the Department of Electrical Engineering, The University of Tokyo, as a Research Associate. He later became an Assistant Professor, an Associate Professor, and, in 2000, a Professor. In 2002, he moved to the Institute of Industrial Science as a Professor in the Information and System Division, and in 2008, to the Department of Advanced Energy, Graduate School of Frontier Sciences, The University of Tokyo. During 1991-1992, he was a Visiting Researcher at the University of California, Berkeley.

His research fields are control theory and its industrial applications to motion control, mechatronics, robotics, electric vehicles, etc. Prof. Hori has been the Treasurer of the IEEE Japan Council and Tokyo Section since 2001. He was the winner of the Best Transactions Paper Award from the IEEE Transactions on Industrial Electronics in 1993 and 2001, of the 2000 Best Transactions Paper Award from the IEEJ.

He is a Member of the IEEE (Fellow), Society of Instrument and Control Engineers, Robotics Society of Japan, Japan Society of Mechanical Engineers, and Society of Automotive Engineers of Japan, etc. He is currently the President of the Industry Applications Society of the Institute of Electrical Engineers of Japan (IEEJ), the President of Capacitors Forum, and the Chairman of Motor Technology Symposium of JMA (Japan Management Association).